

svPITE: A Python package for the state-vector-based probabilistic imaginary-time evolution algorithm

Pascal Sievers^{1,2*} and Satoshi Ejima^{1†}

¹ Institute of Software Technology, German Aerospace Center (DLR), 22529 Hamburg, Germany

² Department of Physics, University of Hamburg, Notkestraße 9-11, 22607 Hamburg, Germany

* pascal.sievers@dlr.de, † satoshi.ejima@dlr.de

Abstract

We present a Python package for ground-state preparation based on the probabilistic imaginary-time evolution algorithm, with particular focus on its state-vector-based implementation. A standard shot-based simulation is also supported, and results can be benchmarked against exact diagonalisation via a dedicated wrapper. The package enables efficient tuning of initial parameters, facilitating systematic exploration and optimisation of the method's performance. Starting from the prepared ground state, the strong interoperability with other packages further enables real-time evolution and the computation of spectral functions, such as the spin-spin dynamical structure factor.

Copyright attribution to authors.

This work is a submission to SciPost Physics Codebases.

License information to appear upon publication.

Publication information to appear upon publication.

Received Date

Accepted Date

Published Date

Contents

1	Introduction	2
2	Overview of the PITE algorithm and its state-vector formulation	3
2.1	PITE algorithm	3
2.2	State-vector formulation	4
3	Package overview	4
3.1	Hamiltonian and operator representation	5
3.2	Configuration object	5
3.3	Algorithm layer	5
3.4	Result objects	6
4	Using svPITE: Basic workflow	6
4.1	Define the Hamiltonian	6
4.2	Algorithm configuration	8
4.3	Running the simulation and accessing the results	8
4.4	Comparison with ED	9
4.5	Beyond the basic workflow: Using the svPITE Output in further simulations	10

5	Examples and benchmarks	11
5.1	Ground-state energy convergence in 1D spin models	11
5.2	Ground-state preparation in a 2D lattice model	13
5.3	Dynamic structure factor of the Heisenberg model	14
6	Future perspectives	15
A	Installation guide	17
A.1	Installing uv	17
A.1.1	MacOS / Linux	17
A.1.2	Windows	17
A.2	Installing svPITE	17
B	Parallelisation and optimisation of state-vector simulations	18
B.1	Parallelisation of real-time evolution	18
B.2	Optimised state-vector evolution	19
B.3	Computational cost of shot-based simulations	20
C	Full Code Examples	21
C.1	State-vector simulation	21
C.2	Shot-based simulation	21
C.3	ED simulation	22
C.4	Hamiltonian construction	23
C.5	Basic workflow example	24
	References	27

1 Introduction

Imaginary-time evolution (ITE) is a central technique in quantum many-body physics, widely used for ground-state preparation and thermal state simulations [1–3]. In recent years, there has been growing interest in implementing imaginary-time dynamics on quantum devices, where non-unitary evolution must be approximated using variational, quantum or probabilistic approaches [4–9].

Probabilistic ITE (PITE) provides one such framework, in which non-unitary evolution $e^{-\hat{H}\Delta\tau}$ is realized via stochastic application of unitary operations combined with measurement and post-selection [7–9]. This approach enables the emulation of imaginary-time dynamics while remaining compatible with the constraints of quantum circuits. While most existing implementations of PITE focus on shot-based realizations that explicitly incorporate sampling and measurement noise, classical simulations based on state-vector representations remain essential for benchmarking and methodological development, as demonstrated in Ref. [10]. In particular, state-vector implementations allow one to isolate intrinsic algorithmic properties such as convergence behaviour and approximation accuracy, independently of statistical fluctuations.

The present codebase provides a reference implementation of PITE using a state-vector backend, while also supporting shot-based simulations within the same framework. It also enables direct comparison with exact diagonalization (ED) results in the same environment,

where ED calculations are performed using QuSpin [11]. It is designed for generic quantum spin systems with up to two-body interactions, allowing users to specify a wide class of Hamiltonians in a flexible manner. The implementation is built on top of Qiskit [12], enabling direct use of its circuit abstraction, simulation tools, and built-in parallelization capabilities. This facilitates efficient execution as well as straightforward extension to hardware-oriented workflows. Compared to existing approaches, the code emphasizes a unified treatment of state-vector and shot-based PITE, providing a transparent environment for cross-validation between idealized and sampling-based dynamics. The modular structure further allows users to explore algorithmic variants and extensions with minimal overhead. The code reproduces the results presented in Ref. [10], and most of the figures can be readily regenerated using the provided scripts. This ensures full reproducibility and facilitates direct comparison with previously reported results.

This paper is organized as follows. Section 2 briefly reviews the theoretical framework of PITE. Section 3 gives an overview of the package. Section 4 describes the basic workflow for using svPITE. Section 5 presents examples and benchmarks, and Section 6 outlines future perspectives.

2 Overview of the PITE algorithm and its state-vector formulation

In this section, we briefly review the PITE algorithm as introduced in Refs. [8, 9] and then outline the state-vector formulation derived in Ref. [10], which underlies the state-vector-based implementation used in this work.

2.1 PITE algorithm

For an initial state $|\psi_{\text{ini}}\rangle$, ITE under Hamiltonian \hat{H} is formally given by

$$|\psi(\Delta\tau)\rangle = \frac{e^{-\hat{H}\Delta\tau}|\psi_{\text{ini}}\rangle}{\|e^{-\hat{H}\Delta\tau}|\psi_{\text{ini}}\rangle\|}, \quad (1)$$

which is non-unitary and thus not directly implementable in a unitary quantum circuit. To circumvent this, we embed the non-unitary operator $\hat{T} \equiv \gamma e^{-\hat{H}\Delta\tau}$ into a larger unitary that acts on the L -qubit system together with a single ancillary qubit. In the ancilla basis $\{|0\rangle, |1\rangle\}$ the unitary has the block form

$$\hat{U}_{\hat{T}} \equiv \begin{pmatrix} \hat{T} & \sqrt{1-\hat{T}^2} \\ \sqrt{1-\hat{T}^2} & -\hat{T} \end{pmatrix}. \quad (2)$$

Here, the parameter γ is initialized at the beginning of the simulation and controls the trade-off between convergence towards the ground state and statistical efficiency of the probabilistic updates. Determining an optimal or near-optimal value of γ is therefore one of the central objectives of svPITE. To describe the action of the unitary, let the ancilla be initialized in $|0\rangle$, and let $|\psi\rangle$ be an arbitrary state of the L -qubit system. The unitary $\hat{U}_{\hat{T}}$ then acts as

$$\hat{U}_{\hat{T}}|\psi\rangle \otimes |0\rangle = \hat{T}|\psi\rangle \otimes |0\rangle + \sqrt{1-\hat{T}^2}|\psi\rangle \otimes |1\rangle \quad (3)$$

thus implementing the non-unitary map \hat{T} probabilistically. Measuring the ancilla qubit in the $|0\rangle$ state, which occurs with probability $\mathbb{P}_0 = \langle\psi|\hat{T}^2|\psi\rangle$, produces the desired state, proportional to $\hat{T}|\psi\rangle$. The complementary outcome applies the Kraus operator $\sqrt{1-\hat{T}^2}$ and the resulting state is discarded.

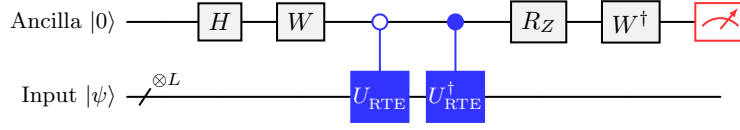


Figure 1: Quantum circuit of the approximate PITE algorithm for a single imaginary-time step. H denotes the Hadamard gate and $R_Z \equiv R_Z(-2\theta_0)$ represents a single-qubit rotation about the Z axis.

Implementing \hat{U}_τ directly would require the operators $\exp(\pm i\kappa\hat{\Theta})$, with $\kappa \equiv \text{sgn}(\gamma - 1/\sqrt{2})$ and $\hat{\Theta} \equiv \arccos\left[\hat{\mathcal{T}} + \sqrt{1 - \hat{\mathcal{T}}^2}/\sqrt{2}\right]$, making an exact realization impractical [8].

Instead, in the small $\Delta\tau$ limit, we expand $\hat{\Theta}$ as $\kappa\hat{\Theta} = \theta_0 - \hat{\mathcal{H}}s_1\Delta\tau + \mathcal{O}(\Delta\tau^2)$, where $\theta_0 \equiv \kappa \arccos[(\gamma + \sqrt{1 - \gamma^2})/\sqrt{2}]$ and $s_1 \equiv \gamma/\sqrt{1 - \gamma^2}$. With that, \hat{U}_τ can be approximated using real-time evolution (RTE) operators $\hat{U}_{\text{RTE}}(\Delta t) \equiv e^{-i\hat{\mathcal{H}}\Delta t}$ and the PITE quantum circuit, which includes the single-qubit gate $W \equiv \frac{1}{\sqrt{2}}\begin{pmatrix} 1 & -i \\ 1 & i \end{pmatrix}$, is constructed as shown in Fig 1.

This circuit represents one imaginary-time step and includes a projective measurement of the ancilla qubit after the step. It is the basis of the package’s shot-based PITE module, where RTE is performed using a Trotter-Suzuki decomposition [13, 14].

Since this shot-based circuit simulation is not the best starting point for simulation and parameter exploration on classical hardware, this package focuses primarily on a state-vector-based formulation of the same approximate PITE update. This formulation avoids explicit ancilla measurements and enables efficient analysis of the evolution and of suitable choices of the parameter γ before running shot-based simulations.

2.2 State-vector formulation

As derived in [10], the approximate PITE algorithm depicted in Fig 1 can be formulated as a state-vector-based simulation. If $|\psi_j\rangle$ is the state after the j th PITE step, the unnormalised wavefunction of the system after the $(j + 1)$ th step followed by a projection of the ancillary qubit on the success state $|0\rangle$ is

$$|\psi_{\text{new}}\rangle = \frac{1}{2\sqrt{2}} \left((1 - i)e^{i\theta_0} \hat{U}_{\text{RTE}}(s_1\Delta\tau) + (1 + i)e^{-i\theta_0} \hat{U}_{\text{RTE}}^\dagger(s_1\Delta\tau) \right) |\psi_j\rangle. \quad (4)$$

The normalised wavefunction after the successful $(j + 1)$ th step is $|\psi\rangle = |\psi_{\text{new}}\rangle/\sqrt{\mathbb{P}_0^{(j)}}$. Here, $\mathbb{P}_0^{(j)} = \langle\psi_{\text{new}}|\psi_{\text{new}}\rangle$ is the conditional probability of success for the $(j + 1)$ th step given that the first, second, \dots , and j th PITE steps were successful as well. This update scheme is implemented in the package’s state-vector-based PITE module.

The state-vector-based PITE simulation does not suffer from statistical uncertainties and corresponds to the infinite-shot limit of the shot-based simulation. Moreover, since it requires neither explicit measurements nor ancillary qubits, the algorithm reduces to a sequence of real-time evolutions. This leads to a substantial improvement in computational efficiency, as demonstrated in later sections using this package.

3 Package overview

The purpose of the svPITE package is to provide a modular, user-friendly Qiskit-based implementation of the PITE algorithm, that integrates into existing workflows. The package implements both the shot-based approach using a single ancillary qubit and the state-vector-based formulation. Additionally, it provides an ED interface via QuSpin for direct comparison.

svPITE is designed to be easy to use for typical workflows while remaining modular and customizable when needed. Users can define custom initial states, provide alternative backends, or specify custom pass managers for the shot-based algorithm, enabling integration with other quantum simulation pipelines. Through its interoperability with QuSpin (for ED simulations) and Qiskit, it complements rather than replaces existing tools.

Conceptually, svPITE is organized into four main building blocks: Hamiltonian and operator representations, configuration objects, the algorithm classes, and structured result objects. This separation ensures a consistent user interface across simulation methods and allows easy extension.

3.1 Hamiltonian and operator representation

All quantum operators in svPITE are represented internally as weighted sums of Pauli strings acting on a fixed number of lattice sites. The fundamental internal data structure is the `PauliStringOperator`, which stores the Pauli labels, site indices, and coefficients of each term. The `Hamiltonian` class is built on top of `PauliStringOperator`, enforcing Hermiticity and providing Hamiltonian-specific methods. This abstraction ensures that both high-level model classes (e.g. Ising and Heisenberg models in one and two dimensions) as well as user-defined Hamiltonians are expressed in this common internal format used by all three simulation techniques.

At present, the `Hamiltonian` class supports single-site terms and two-site $X_i X_j$, $Y_i Y_j$, and $Z_i Z_j$ couplings. More general mixed Pauli terms, such as $X_i Y_j$, are supported at the level of `PauliStringOperator`, but not yet by the `Hamiltonian` interface.

Both `PauliStringOperator` and `Hamiltonian` instances can be converted to a Qiskit `SparsePauliOp`, and `Hamiltonian` instances can additionally be translated into QuSpin `Hamiltonians`.

3.2 Configuration object

The configuration objects (`PITEConfig` and `EDConfig`) are lightweight dataclasses that collect all algorithm parameters (e.g. γ , $\Delta\tau$, Trotter order, number of steps, shot count, and the choice of initial state) into a single validated structure. They make simulations reproducible, provide a common configuration interface across all three algorithms, and help avoid common input mistakes. Together with the `Hamiltonian`, the configuration fully specifies the input to each algorithm.

3.3 Algorithm layer

Given a `Hamiltonian` and the corresponding configuration object, the algorithm classes carry out the simulation. The `PITEStatevector` and `PITEShot` classes implement the state-vector-based and shot-based PITE algorithms discussed in Sec. 2, respectively, while the `ED` class provides an exact-diagonalisation reference for the PITE simulations.

The `ED` algorithm class serves as a thin wrapper around the QuSpin package [11]. Using the parameters specified in the `EDConfig`, QuSpin is employed to construct the appropriate spin-chain basis. The svPITE `Hamiltonian` is then translated into the corresponding QuSpin operator representation, and the ground-state energy and corresponding eigenvector are obtained via QuSpin's sparse exact-diagonalisation routines. The resulting ground state serves as a benchmark for the PITE implementation and is used to validate and calibrate PITE parameters.

3.4 Result objects

For each algorithm, the simulation output is returned as a dedicated result object, namely, `PITEStatevectorResult`, `PITESHOTResult`, or `EDResult`, which stores the results in a structured form. These objects provide relevant observables such as energies and success probabilities, which can be directly used for analysis and plotting. In addition, they store the configuration used for the simulation, and can optionally include the generated circuit or final state. This separation also allows additional outputs to be added without changing the user-facing workflow.

4 Using svPITE: Basic workflow

To demonstrate how svPITE can be used, this section walks through a standard workflow step by step. We assume that the package is installed and that the reader is familiar with basic Python. The installation can be performed easily using the `uv` package manager, and a detailed guide is provided in App. A. We will also assume that all necessary imports are in place. The three primary algorithms are available as top-level imports, while configurations, results, operators, and Hamiltonian models are imported from dedicated submodules:

```
# ---- Importing everything ----
# Algorithms
from svpите import PITEStatevector, PITESHOT, ED

# Configurations
from svpите.configs import PITEConfig, EDConfig

# Operators and Hamiltonians
from svpите.operator import PauliStringOperator, Hamiltonian

# Specific models
from svpите.operator.models import (
    IsingHamiltonian, HeisenbergHamiltonian,
    XYHamiltonian, XXZHamiltonian
)
```

We will consider a concrete physical system and walk through the workflow of obtaining the ground state using state-vector-based PITE, shot-based PITE, and ED, allowing for a comparison of the results. By explaining every step in detail, we aim to familiarize the reader with the usage of the package. At the end of the section, we will also demonstrate the usage beyond computing the ground state. The complete code, including the necessary imports and the scripts used to generate the figures, is provided in App. C.

4.1 Define the Hamiltonian

As an example, we consider the XXZ Heisenberg Hamiltonian in a longitudinal magnetic field, defined as

$$\hat{\mathcal{H}} = J \sum_{j=0}^{L-1} (\hat{X}_j \hat{X}_{j+1} + \hat{Y}_j \hat{Y}_{j+1} + \Delta \hat{Z}_j \hat{Z}_{j+1}) + h_z \sum_{j=0}^{L-1} \hat{Z}_j. \quad (5)$$

Here, \hat{X}_j , \hat{Y}_j , and \hat{Z}_j denote Pauli operators acting on site j . The coupling constant J sets the overall interaction scale, Δ controls the anisotropy, and h_z denotes the strength of the external field in z -direction. The system consists of L sites labeled by $j = 0, 1, \dots, L-1$. We assume

periodic boundary conditions (PBC) by identifying site L with site 0, i.e., $\hat{O}_L \equiv \hat{O}_0$ for all local operators \hat{O} .

As a first step, we start by defining the physical model parameters:

```
import numpy as np
# ---- Define model parameters ----
L = 8 # number of lattice sites
J = 1.0 / 4.0 # coupling constant
Delta = 1.0 / np.sqrt(2.0) # anisotropy
hz = 1.0 / 5.0 # external field
bc = 'PBC' # periodic boundary conditions
```

To define the Hamiltonian $\hat{\mathcal{H}}$ from Eq. (5), we use the predefined XXZ model included in the package as a starting point. By passing in the boundary conditions, the two-site terms are automatically constructed in the correct way. Note that, since operators are internally represented as Pauli strings, all methods for initializing operators use Pauli operators. To work with spin operators, one can simply use the relation $\hat{S}_i^\alpha = \frac{1}{2}\hat{P}_i^\alpha$ for $\hat{P}^\alpha \in \{\hat{X}, \hat{Y}, \hat{Z}\}$ and absorbs the corresponding factors of $1/2$ into the model parameters.

```
# ---- Define XXZ Hamiltonian in external z-field ----
# Use standard XXZ model as starting point
H = XXZHamiltonian(L, J, Delta, bc)
```

For standard spin models, this is the recommended and easiest way to start. Alternatively, especially for non-standard models, one can provide a dictionary of coefficient arrays (`terms_dict`) to the Hamiltonian constructor, allowing full control over couplings and lattice structure. Specifically, the dictionary uses strings specifying Pauli operator combinations (e.g. "Z", "XX", "ZZ") as keys, and one- or two-dimensional arrays as values corresponding to single-site or two-site coupling strengths, respectively. The array entries encode the spatial structure of the interaction, i.e. which sites are coupled and with what strength. For two-site terms, the coupling array has the form J_{ij} where each non-zero entry specifies an interaction between site i and site j . The XXZ model with PBC can therefore be defined as:

```
# Alternatively: Full manual construction
J_xy, J_z = np.zeros((L, L)), np.zeros((L, L))
for i in range(L):
    J_xy[i, (i+1)%L] = J
    J_z[i, (i+1)%L] = J * Delta
terms_dict = {"XX": J_xy, "YY": J_xy, "ZZ": J_z}
H = Hamiltonian(L, terms_dict)
```

Additional Hamiltonian construction methods and further examples are provided in App. C. In all cases, the resulting Hamiltonian instance can be passed directly into the PITE algorithm. In our example, the external field still needs to be added, which can be done using the `add_uniform_terms` method that adds a translationally invariant term to the Hamiltonian.

```
# Add external z-field terms to the Hamiltonian
H.add_uniform_terms("Z", hz)
```

Since we are only adding a single-site term, it is not necessary to specify boundary conditions. In principle, the same term could also be constructed manually, but `add_uniform_terms` provides a more convenient interface for translationally invariant fields. To verify a correct construction, the Hamiltonian can be displayed using `print(H)`, yielding:

$$0.25 * \sum_i X_i X_{i+1} + 0.25 * \sum_i Y_i Y_{i+1} + 0.2 * \sum_i Z_i + 0.177 * \sum_i Z_i Z_{i+1} \text{ (Sums using PBC)}$$

As with the whole package, this representation assumes a one-dimensional (1D) spin chain. Two-dimensional (2D) systems are treated by mapping them onto an effective 1D representation. As a result, their printed representation is not easily readable.

4.2 Algorithm configuration

Having initialized the Hamiltonian, we can now turn to the configuration of the algorithm. Since the ED implementation is merely a wrapper around standard QuSpin with a Hamiltonian translation layer that is intended primarily for comparison, we focus here on using the two PITE implementations. Some comments on the usage of the ED wrapper are included in Sec. 4.4.

Both variants of the PITE algorithm require the same configuration object, `PITEConfig`, to specify the algorithm parameters. We can therefore initialize a single configuration object and use it for both algorithms in our comparison. The value of `gamma` used here was determined as described in Sec. 5.1.

```
# ---- Define algorithm parameters ----
config = PITEConfig(
    gamma=0.72, # Gamma parameter of the PITE algorithm
    n_steps=80, # Number of imaginary-time evolution steps
    dt=0.2, # Imaginary-time step size
    order=1, # Trotter order for the real-time evolution gate
    initial_state='singlet', # Initial state of the evolution
    n_shots=10000, # Number of shots for shot-based PITE
)
```

Supported initial states are 'zero', 'one', 'random', 'plus', 'minus', 'neel', and 'singlet'. Alternatively, users may provide a Qiskit `Statevector` or `QuantumCircuit` to specify a custom initial state with greater overlap with the expected ground state, thereby accelerating convergence. The parameter `n_shots` is optional and is ignored when the configuration is used for a state-vector-based simulation.

4.3 Running the simulation and accessing the results

All necessary ingredients for performing the PITE simulations have now been introduced. The interfaces of the shot-based and state-vector-based implementations are nearly identical, differing only in optional execution parameters. A simulation is run by initializing the algorithm class with the Hamiltonian and configuration and then calling the `run()` method:

```
# ---- Initialize and run algorithms ----

# Statevector PITE
sv_algorithm = PITEStatevector(config, H)
sv_result = sv_algorithm.run(verbose=True, return_statevector=True)

# Shot-based PITE
shot_algorithm = PITEShot(config, H)
shot_result = shot_algorithm.run(verbose=True, return_circuit=False)
```

By setting `verbose=True`, the progress of the simulation will be printed during execution. The flag `return_statevector` adds the final state-vector to the result object for inspection, comparison or further use, while `return_circuit` adds the circuit of the first PITE iteration (including the state preparation) to the result object. This can be useful for analysis or optimisation.

The shot-based simulation additionally supports more advanced backend options such as `use_primitives`, `optimization_level`, and `pass_manager`, which allow fine-grained control over transpilation, execution, and sampling. Here we will rely on the default values and not discuss these options further, as they are part of Qiskit's execution and transpilation framework.

Both calls return result objects that store all relevant observables together with the configuration used for the simulation, and can be printed directly for a short summary. The state-vector result (`sv_result`) provides the energy and success probability at each step without sampling noise, whereas the result of the shot-based simulation (`shot_result`) only provides the success probability at each step. The energy in the shot-based simulation is measured only after the final step and returned together with its statistical standard deviation.

```
# ---- Access and print results ----
print(sv_result)
print(shot_result)

# Statevector PITE results
E_sv = sv_result.energies # Energy per site vs PITE step
P_sv = sv_result.proBABILITIES # Success probabilities vs PITE
    step

# Shot-based PITE results
E_shot = shot_result.energy # Final energy per site
dE_shot = shot_result.energy_std # Standard deviation of final
    energy per site
P_shot = shot_result.proBABILITIES # Success probabilities vs
    PITE step
```

The state-vector result includes the final state via `sv_result.final_statevector`, which will be used later. If requested, the first-iteration circuit of the shot-based simulation would be accessible through `shot_result.circuit`.

4.4 Comparison with ED

To establish a reference ground state of our example system, we can use the QuSpin ED integration with the same Hamiltonian \hat{H} . The setup closely parallels the PITE workflow, but uses an `EDConfig` instance instead. This configuration can specify symmetry sectors through QuSpin basis arguments, as well as optional `eigsh()` eigensolver parameters:

```
# ---- Reference ED calculation ----
# Define ED configuration with symmetry sectors for the ground
    state computation
ed_basis_kwargs = {"Nup": L//2, "pblock": 1, "kblock": 0}
ed_config = EDConfig (
    tol = 1e-10, # Tolerance for eigensolver
    maxiter = 1e4, # Maximum iterations for eigensolver
    v0 = None, # Initial vector for eigensolver
    spin_basis_1d_kwargs = ed_basis_kwargs
)
```

For details on the symmetry sector definitions and eigensolver options, consult the [QuSpin documentation](#).

Running ED is analogous to running the PITE simulations. The ED call also returns a result object that stores the ground state energy together with the simulation configuration, and optionally the ground-state vector.

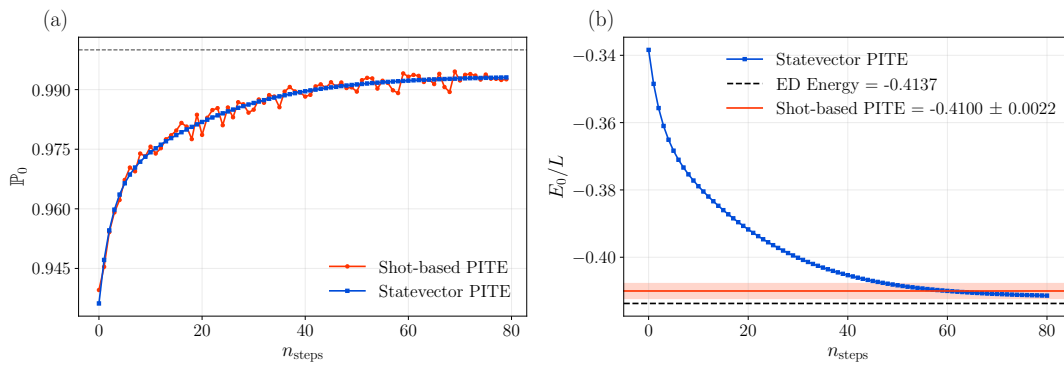


Figure 2: (a) Success probability \mathbb{P}_0 as a function of imaginary time steps n_{steps} for the state-vector-based (blue) and shot-based (red) implementations of the PITE algorithm, obtained using the example code provided in this section. (b) Corresponding energy per site E_0/L as a function of n_{steps} for the state-vector-based simulation, as well as the final energy estimate from the shot-based PITE simulation including its standard deviation. The exact ground-state energy per site obtained by ED is shown as a black dashed line.

```
# Initialize and run ED algorithm
ed_algorithm = ED(ed_config, H)
ed_result = ed_algorithm.run(verbose=True, return_groundstate=False)

# Access ED results
print(ed_result)
E_ed = ed_result.energy # Computed ground state energy
```

Figure 2 compares the results obtained with the example code using the state-vector-based and shot-based PITE simulations, along with the ED reference. The computation was performed in approximately 2 minutes on a MacBook Pro with an Apple M1 Max processor. The full code, including the plotting routines, is provided in App. C.

4.5 Beyond the basic workflow: Using the svPITE Output in further simulations

A converged state from the state-vector-based PITE implementation is not limited to ground-state preparation but can serve as the starting point for further simulations. In particular, it can be used within the Qiskit ecosystem or in custom simulation workflows to study, for example, quenches, real-time expectation values, or correlation functions.

The final state returned by `PITEStatevector` can be directly combined with Qiskit's native state-vector tools and circuit objects. For instance, an svPITE Hamiltonian can be translated into a Qiskit real-time evolution circuit, allowing one to evolve the prepared state under the same Hamiltonian:

```
# Get final statevector from the results
psi0 = sv_result.final_statevector

# Real-time evolution generated by H
U_dt = H.to_time_evolution_circuit(dt=1/100, reps=100, order=1)

# Apply the evolution circuit to the prepared state
from svpите import evolve_statevector
psi_t = evolve_statevector(psi0, U_dt)
```

Here, we used our optimised `evolve_statevector()` function instead of the standard Qiskit method. For more details, see App. B.

Expectation values of observables can then be evaluated at different times using standard Qiskit functionality. For example, given an operator O in the package representation, one may convert it to a `SparsePauliOp` and evaluate its expectation value:

```
O_qiskit = O.to_sparse_pauli_op()
value_t = psi_t.expectation_value(O_qiskit)
```

Repeating this for a sequence of times yields time-dependent observables such as $\langle \hat{O}(t) \rangle$.

While the Qiskit interface provides a convenient way to continue working with the PITE output, the full wavefunction returned by `PITEStatevector` can also be accessed directly through `psi0.data`. This exposes the underlying NumPy array and enables post-processing outside of Qiskit. Likewise, operators represented in svPITE can not only be converted into Qiskit operators, but also to matrix form:

```
# Access full statevector as NumPy array
psi_np = psi0.data

# Convert operator to sparse matrix
O_mat = O.to_matrix(sparse=True)

# Example: expectation value using NumPy
value = np.vdot(psi_np, O_mat @ psi_np)
```

We use this functionality in Sec 5.3 to compute the dynamic structure factor of the Heisenberg model.

5 Examples and benchmarks

This section presents a set of application examples that demonstrate how svPITE can be used in practical simulations. We illustrate ground-state preparation in one- and two-dimensional spin-models, including parameter selection and convergence behaviour. Furthermore, we show how the resulting states enable further studies, including real-time dynamics and spectral functions. These examples provide a practical reference and benchmark for the PITE implementations.

5.1 Ground-state energy convergence in 1D spin models

First, we demonstrate how to determine the initial parameter set, $\Delta\tau$ and γ , for spin models. As an example, we consider the 1D Heisenberg model, which corresponds to Eq. (5) with $\Delta = 1$ and $h_z = 0$. As before, we assume PBC. Throughout this section, we also set $J = 1/4$ to define the energy unit.

To determine a suitable value γ , a sweep of state-vector simulations is performed over different values of γ for a fixed $\Delta\tau$. By repeating this procedure for different choices of $\Delta\tau$ and comparing the results, a suitable set of parameters can be identified.

Figure 3 shows such a sweep for a system with $L = 16$ sites and $\Delta\tau = 0.2$. The convergence of the approximate ground-state energy per site E_0/L and success probability \mathbb{P}_0 illustrates the trade-off between accuracy and success probability. If the exact ground state is available, the infidelity $1 - F = 1 - |\langle \psi_{\text{ED}} | \psi_{\text{svPITE}} \rangle|^2$ provides an additional accuracy measure for the approximate state, complementing the energy-based estimate. As shown in panels (b)

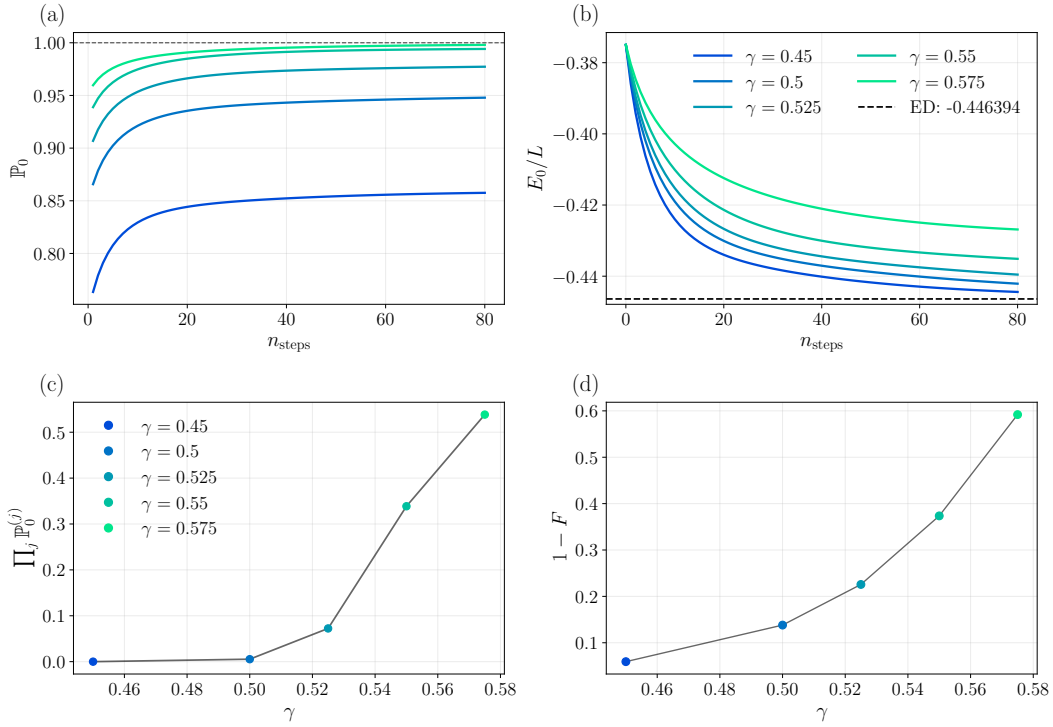


Figure 3: State-vector PITE simulations for different values of γ for the spin-1/2 Heisenberg chain with $L = 16$, using a singlet initial state and $\Delta\tau = 0.2$ with a first-order Trotter decomposition. (a) Single-step postselection success probability \mathbb{P}_0 and (b) approximate ground-state energy per site E_0/L as functions of the number of imaginary-time steps n_{steps} (i.e., PITE steps) for each γ . The exact ground-state energy E_{ED}/L is shown as a dashed horizontal line. (c) Cumulative success probability $\prod_j \mathbb{P}_0^{(j)}$ and (d) infidelity $1 - |\langle \psi_{\text{ED}} | \psi_{\text{svPITE}} \rangle|^2$ as a function of γ . The script used to generate this figure is available in `examples/heisenberg_gamma_sweep.py`.

and (d), the accuracy can be improved by reducing γ slightly below γ_{max} , which is approximately 0.58 in the present case and yields an almost perfect success probability ($\mathbb{P}_0 \sim 1$), as shown in panel (a). However, this improved accuracy comes at the cost of a lower success probability, which substantially increases the number of required shots. For instance, in shot-based simulations, the fraction of surviving shots after 80 imaginary-time steps is estimated to be less than 10% for $\gamma \leq 0.525$; see panel (c). Thus, in the relevant parameter regime, there is a trade-off between accuracy and success probability, and γ should be chosen to achieve an acceptable balance.

For this example, we choose $\gamma = 0.53$ to perform a shot-based simulation, as it offers good accuracy while maintaining a cumulative success probability above 10%. Figure 4 compares the results of the shot-based simulations with those of the state-vector simulation. For both the success probability and the energy convergence, we find good agreement between the two approaches. As expected, increasing the number of shots leads to closer agreement with the state-vector result, corresponding to the infinite-shot limit without statistical errors. For a discussion of the computational cost of shot-based simulations as compared with the state-vector approach, see App. B.3.

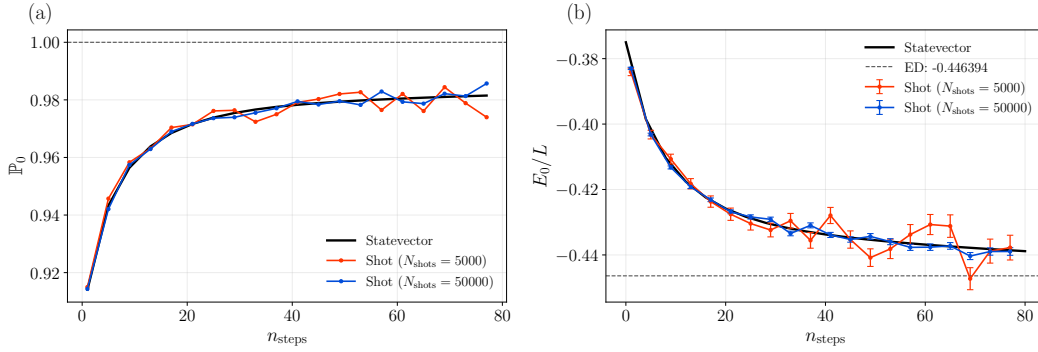


Figure 4: (a) Success probability \mathbb{P}_0 and (b) approximate ground-state energy per site E_0/L as functions of the number of steps, obtained using the shot-based PITE implementation with $\gamma = 0.53$ chosen from Fig. 3. The simulations are performed for the spin-1/2 Heisenberg chain with $L = 16$, using a singlet initial state and $\Delta\tau = 0.2$. Results obtained with 5,000 shots are shown in red and with 50,000 shots in blue. The solid black line indicates the state-vector PITE reference, while the dashed horizontal line denotes the ED energy. The plot was produced using the scripts in `examples/heisenberg_shot_vs_sv/`.

5.2 Ground-state preparation in a 2D lattice model

The PITE algorithm can be directly applied to higher-dimensional systems, where it may offer potential quantum advantage, particularly in applications to condensed matter physics and materials science. To illustrate its performance in such settings, we consider the Heisenberg model on a $L \times L$ square lattice with PBC, defined as

$$\hat{\mathcal{H}}_{\text{Heisen2D}} = J \sum_{\langle i,j \rangle} (\hat{X}_i \cdot \hat{X}_j + \hat{Y}_i \cdot \hat{Y}_j + \hat{Z}_i \cdot \hat{Z}_j), \quad (6)$$

where $\langle i, j \rangle$ denotes nearest-neighbor pairs.

Figure 5 shows the svPITE results in the model (6) using $L = 4$, i.e. $N = 16$ sites. By tuning the initial parameter γ to $\gamma = 0.6$ for fixed $\Delta\tau = 0.1$, the state evolved from a Néel initial state converges to the exact ground state [dashed line in panel (a)] as the number of imaginary-time steps increases. Note that the ground-state energy per site of the 4×4 Heisenberg model

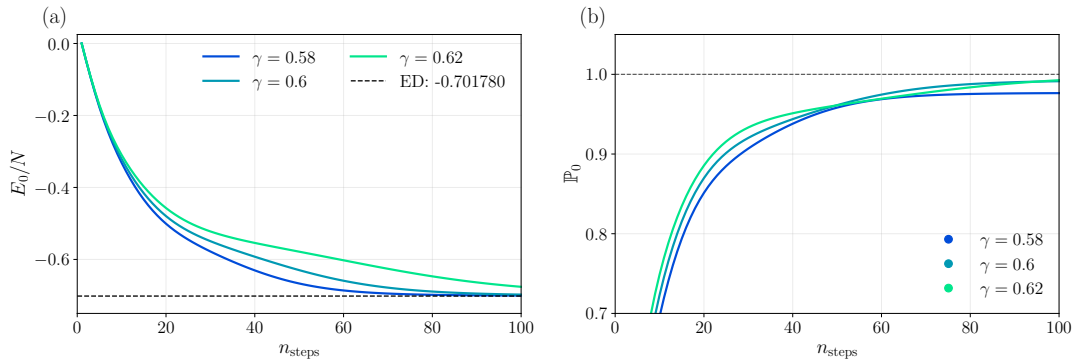


Figure 5: (a) Energy per site E_0/N and (b) success probability \mathbb{P}_0 as functions of imaginary-time steps, n_{step} , obtained with the state-vector-based PITE algorithm in the 2D Heisenberg model on a 4×4 square lattice (i.e., $N = 16$ sites) with PBC. These plots were generated using the script `examples/heisenberg_2d_ed_sv.py`.

obtained by ED is $E_0/N = -0.701780$; see, e.g., Ref. [15]. For these parameter sets, the success probability \mathbb{P}_0 remains close to unity, as desired [see Fig. 5(b)]. For the finite systems considered here, the excitation gap per site is larger in the 4×4 cluster than in the $L = 16$ chain. This larger finite-size gap is consistent with the faster convergence of PITE in two dimensions.

On fault-tolerant quantum computers with a sufficiently large number of logical qubits, reproducing the high-precision Quantum Monte Carlo (QMC) energies of the 2D square-lattice Heisenberg model by PITE would provide an excellent and nontrivial benchmark. In particular, the recent QMC study of the periodic $L \times L$ system has reported highly accurate finite-size energy data up to $L = 96$, offering a valuable reference for assessing the performance of PITE beyond ED system sizes [16].

5.3 Dynamic structure factor of the Heisenberg model

As demonstrated above, the ground state can be systematically determined in both one and two dimensions using svPITE. Theoretically, real-time evolution can then be performed on the obtained ground state to compute dynamical correlation functions (e.g., with the help of the Hadamard test). Spectral functions, such as the dynamic structure factor, can be obtained via Fourier transform. However, realizing such simulations on real devices remains challenging due to the required circuit depth. Nevertheless, in this subsection, we provide illustrative examples of spectral functions obtained using svPITE.

In 1D spin systems, the dynamic spin structure factor is defined as

$$S(q, \omega) = \int_{-\infty}^{\infty} dt \sum_r e^{i(qr - \omega t)} \langle \hat{S}_{j+r}^z(t) \hat{S}_j^z(0) \rangle. \quad (7)$$

In the following, we describe the computational procedure for computing $S(q, \omega)$ using svPITE, step by step. First, we prepare the ground state $|\psi_0\rangle$ by PITE or ED algorithms as explained in Sec. 5.1. In order to compute the time-dependent correlation functions in Eq. (7), we then act with a local spin operator \hat{S}_j^z on the ground state and prepare the initial state $|\phi(0)\rangle = \hat{S}_j^z |\psi_0\rangle$. This state is evolved in real time as $|\phi(t)\rangle = e^{-i\hat{H}t} \hat{S}_j^z |\psi_0\rangle$, where $t = n\Delta t$ and Δt is a small time step. (See Sec. 4.5 for the time-evolution procedure using `evolve_statevector()` in this package.) The dynamical spin correlation function is then evaluated as

$$C^{zz}(r, t) = e^{iE_0 t} \langle \psi_0 | \hat{S}_{j+r}^z e^{-i\hat{H}t} \hat{S}_j^z | \psi_0 \rangle. \quad (8)$$

Finally, the momentum- and frequency-resolved dynamical structure factor, $S(q, \omega)$, is obtained by performing the space-time Fourier transform of $C^{zz}(r, t)$.

Figure 6 shows the obtained results for $S(q, \omega)$ in the Heisenberg chain, corresponding to the XXZ Hamiltonian in Eq. (5) with $\Delta = 1$ and $h_z = 0$, for system size $L = 24$ and PBC. Starting from the ground state obtained with the optimal $\gamma = 0.46$ for fixed $\Delta\tau = 0.2$ and evolving the system in real time with the time step of $\Delta t = 0.025$, $S(q, \omega)$ becomes asymmetric due to the inaccuracy of the ground state as shown in Fig. 6(a), although it should be symmetric about $q = \pi$ as demonstrated by the ED results in Fig. 6(c). This asymmetry can be reduced by using a more accurate ground state obtained with $\gamma = 0.41$, as shown in Fig. 6(b); however, the success probability after 200 imaginary-time steps decreases from 99.9% for $\gamma = 0.46$ to 96.3% for $\gamma = 0.41$, suggesting that a larger number of shots would be required in shot-based simulations.

We would like to note that the code for reproducing Fig. 6 is available as `examples/heisenberg_RTE_ed.py` and `examples/heisenberg_RTE_sv.py`, for the ED and state-vector PITE algorithms, respectively.

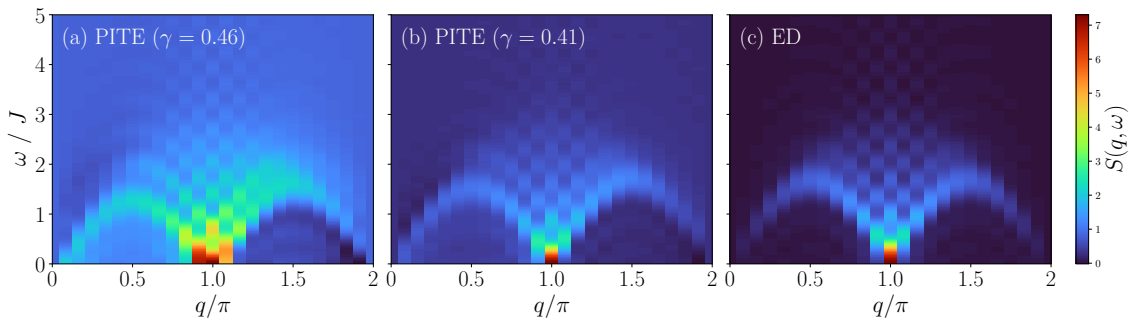


Figure 6: Dynamic structure factor $S(q, \omega)$ with $L = 24$ and PBC in the Heisenberg model, obtained using svPITE. Panels (a) and (b) show results obtained using the state-vector-based PITE algorithm with $\gamma = 0.46$ and 0.41 , respectively, while panel (c) shows results obtained using the ED algorithm.

6 Future perspectives

Several directions for future development could further broaden the applicability and performance of the svPITE package.

A first important extension concerns the treatment of more general interaction structures. At present, the software is well suited to non-mixed interaction terms up to the two-body level, but many physically relevant models involve mixed interaction terms or higher-order many-body contributions. Supporting mixed interaction terms in a more flexible and automated manner would significantly enlarge the class of systems that can be studied within a unified workflow. In particular, a generalized term-handling interface could simplify the implementation of composite Hamiltonians and make the framework more useful for realistic many-body applications.

A second major direction concerns computational efficiency and backend flexibility. In particular, a more detailed investigation is needed into the extent to which efficient parallelisation can be achieved for state-vector-based simulations at larger qubit numbers, where the computational overhead grows rapidly. Clarifying this point will be important for assessing the practical scalability of the current implementation. Although the current implementation relies on Qiskit, it would also be of interest to examine alternative platforms such as Qrisp [17], Cirq/qsim [18], Qulacs [19], PennyLane Lightning [20], or CUDA-Q, and to assess how these choices influence the efficiency and practicality of parallelised state-vector-based simulations at larger qubit numbers.

From a physics perspective, an especially relevant next step is the extension of the present framework to spin systems at finite temperature. While the current implementation focuses on ground-state-oriented or zero-temperature settings, many important questions in condensed-matter and statistical physics require access to thermal observables and finite-temperature states. Incorporating suitable purification schemes, thermal-state preparation strategies, or imaginary-time techniques adapted to mixed states would open the way to a wider range of applications.

Another natural target is the study of Fermi–Hubbard models. These models are among the central benchmarks in quantum simulation and are directly relevant for strongly correlated fermionic systems. However, extending PITE towards fermionic lattice Hamiltonians would require robust support for fermion-to-qubit mappings, efficient treatment of nonlocal operator strings, and careful optimisation of measurement costs. Achieving this would considerably strengthen the scientific scope of the software and connect it to a broad body of ongoing work in quantum many-body physics.

Overall, future development should proceed along two complementary lines: expanding the range of physical models to include mixed interactions, finite-temperature spin systems, and fermionic models such as the Fermi–Hubbard Hamiltonian, while also improving the software architecture through enhanced parallelisation on both traditional HPC systems and GPU-based platforms. Together, these developments would make svPITE a more versatile and sustainable platform for quantum simulation research.

Acknowledgements

SE acknowledges the Q-Neko project, which has received funding from the European Union’s Horizon Europe research and innovation programme under Grant Agreement No. 101241875. This work was also performed for Council for Science, Technology and Innovation (CSTI), Cross-ministerial Strategic Innovation Promotion Program (SIP), “Promoting the application of advanced quantum technology platforms to social issues”(Funding agency: QST).

This project was made possible by the DLR Quantum Computing Initiative and the Federal Ministry for Economic Affairs and Climate Action; qci.dlr.de/projects/ALQU.

The authors gratefully acknowledge the scientific support and HPC resources provided by the German Aerospace Center (DLR). The HPC system CARO is partially funded by "Ministry of Science and Culture of Lower Saxony" and "Federal Ministry of Research, Technology and Space".

A Installation guide

svPITE and its dependencies can be installed using the package and project manager `uv`. The package depends on `QuSpin` and `Qiskit` and is tested with Python 3.11 and 3.12. All required dependencies are specified in the project configuration `pyproject.toml` and are installed automatically (including a compatible Python version) when following the minimal installation procedure below. The use of `uv` ensures a simplified setup of reproducible environments and provides unified dependency and Python version management.

A.1 Installing `uv`

`uv` can be installed as a standalone binary without requiring an existing Rust or Python installation. For more detailed information, refer to the official [uv documentation](#).

A.1.1 MacOS / Linux

```
$ curl -LsSf https://astral.sh/uv/install.sh | sh
$ uv --version
```

Alternatively, `uv` can be installed from [PyPI](#) using `pip` or `pipx`, or via [Homebrew](#) on macOS. If installed using the standalone script, `uv` can be updated by running `uv self update`; otherwise, updates are handled by `pip` or `brew`.

A.1.2 Windows

```
> powershell -ExecutionPolicy Bypass -c "irm https://astral.sh
/uv/install.ps1 | iex"
> uv --version
```

A.2 Installing svPITE

The installation procedure is identical on Windows, macOS, and Linux. Clone the repository and run `uv sync` to install all dependencies:

```
$ git clone https://gitlab.com/quantum-computing-software/
  svpите
$ cd svpите
$ uv sync
```

This creates a dedicated virtual environment `.venv` inside the package directory and installs all dependencies specified in `pyproject.toml`. Existing Python installations are not affected.

To install additional dependencies required for some example scripts and notebooks:

```
$ uv sync --group examples
```

More detailed usage guidance for `uv` (e.g., adding packages, updating environments) is available in the project `README` and in the `uv` documentation.

Any Python script can now be executed using `uv run`:

```
$ uv run examples/ising_4_sv.py
```

Alternatively, the virtual environment can be activated manually:

```
# On macOS and Linux
$ source .venv/bin/activate
```

```
# On Windows
> .\.venv\Scripts\activate
```

When the environment is active, Python commands and package installations affect only this environment.

B Parallelisation and optimisation of state-vector simulations

To optimise the state-vector-based PITE simulation and thereby accelerate parameter exploration, we implemented two main strategies: (i) parallel simulation of the real-time evolution \hat{U}_{RTE} and its Hermitian adjoint $\hat{U}_{\text{RTE}}^\dagger$, and (ii) a custom state-vector evolution routine tailored specifically to the operators used in the PITE algorithm. By combining these two optimisations, we achieve an overall speedup of approximately $2\times$ for systems with $L \geq 22$ sites.

All benchmark results presented in this section were obtained using the scripts available in `examples/sv_evolve_benchmarks/`.

B.1 Parallelisation of real-time evolution

Computing the updated state-vector according to Eq. (4) involves a linear combination of forward- and backward-time evolution operators acting on the current state. The application of these two operators can therefore be evaluated in parallel. This behaviour can be controlled via the `parallel_evolve` parameter of the state-vector `run()` function. It is enabled by default, as it provides a speedup for systems larger than $L \gtrsim 12$.

For smaller systems, however, the overhead associated with process synchronisation after each step outweighs the benefit of parallelisation, as shown in Fig. 7. The speedup approaches $\sim 1.6\times$ for large systems and does not depend on the number of PITE steps, since both evolution branches are evaluated independently at each step (see Fig. 8).

Our benchmarks were performed on a MacBook Pro equipped with an Apple M1 Max processor. The exact speedup and the crossover system size depend on the specific hardware and software environment.

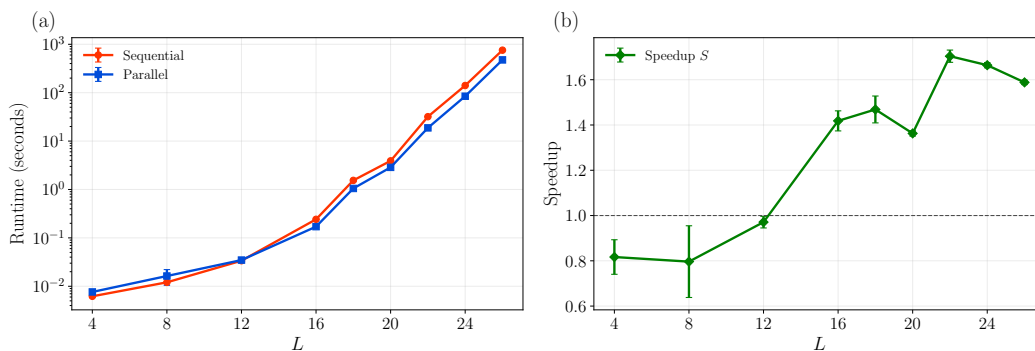


Figure 7: (a) Runtime of state-vector PITE simulations using sequential and parallel evolution as a function of system size L for a fixed number of steps, $n_{\text{steps}} = 10$. (b) Corresponding speedup, $S = t_{\text{seq}}/t_{\text{par}}$. The data correspond to a Heisenberg chain. Error bars show the standard deviation over 10 simulations per data point.

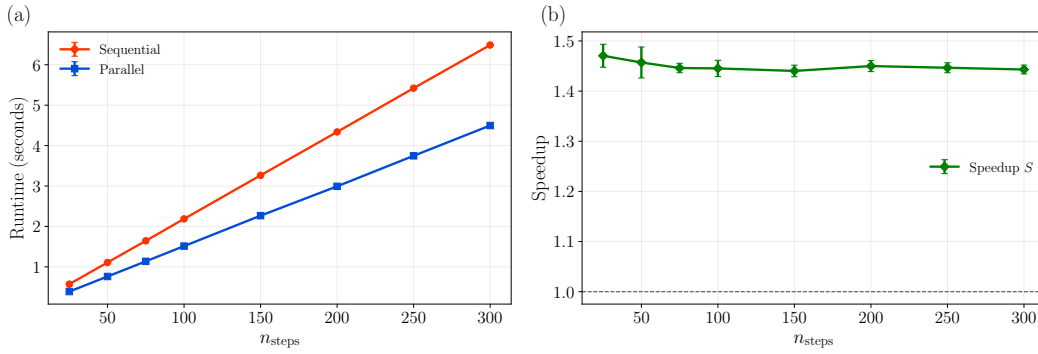


Figure 8: (a) Runtime of state-vector PITE simulations using parallel and sequential evolution as a function of the number of steps n_{steps} , and (b) the corresponding speedup, $S = t_{\text{seq}}/t_{\text{par}}$. The test was performed for a Heisenberg chain with $L = 16$ sites. Error bars show the standard deviation over 10 simulations per data point.

B.2 Optimised state-vector evolution

Since the time-evolution circuit used in svPITE is always constructed from a `SparsePauliOp`, the standard `evolve()` function provided by Qiskit can be specialised to this case. By eliminating unnecessary `reshape()` operations, we achieve an additional speedup of $\sim 1.2\times$, independent of system size and the number of time steps (see Figs. 9 and 10).

The use of the custom optimised evolution routine is enabled by default and can be disabled by passing `use_qiskit_evolve=True` to the `run()` function.

Our `evolve_statevector()` function can also be used independently of the PITE algorithm to perform real-time evolution, as demonstrated in Sec. 4.5.

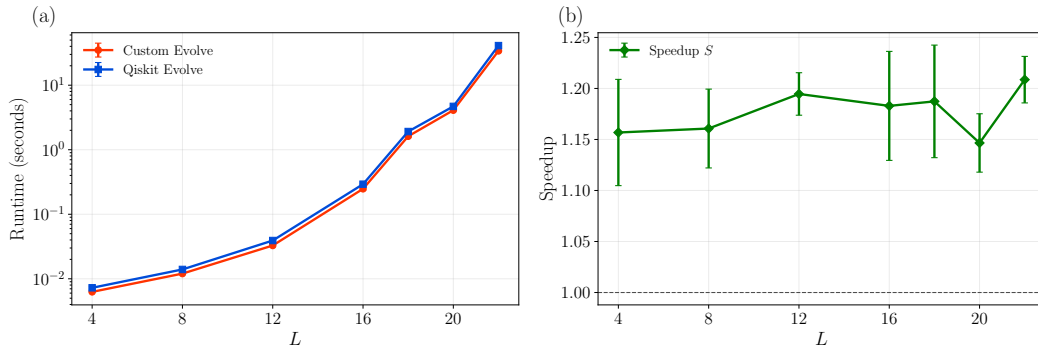


Figure 9: (a) Runtime of state-vector PITE simulations using the custom evolution routine and the Qiskit `evolve()` method as a function of the number of PITE steps n_{steps} , and (b) the corresponding speedup. The test was performed for a Heisenberg chain with $L = 16$ sites. Error bars show the standard deviation over 10 simulations per data point.

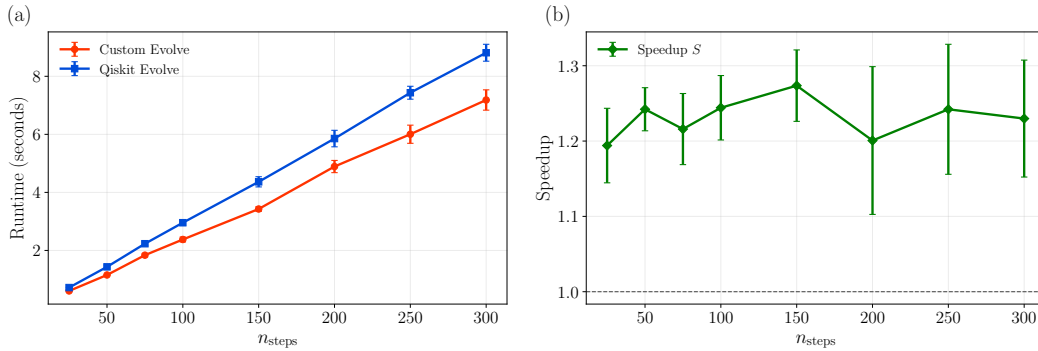


Figure 10: (a) Runtime of state-vector PITE simulations using the custom evolution routine and the Qiskit `evolve()` method as a function of the number of steps n_{steps} , and (b) the corresponding speedup. The test was performed for a Heisenberg chain with $L = 16$ sites. Error bars show the standard deviation over 10 simulations per data point.

B.3 Computational cost of shot-based simulations

While the state-vector PITE algorithm for an $L = 16$ Heisenberg chain can be executed in seconds on a laptop (see Fig. 10), a shot-based simulation requires several hours on a 128-core workstation. Figure 11 shows the corresponding runtimes. As shown in Fig. 4, approximately 50,000 shots are required to obtain a statistically reliable estimate, resulting in a total runtime of ~ 2.5 hours for 80 steps on a 128-core workstation. Moreover, each energy data point requires an independent simulation, since the energy is only measured after the final step. Consequently, obtaining the full energy convergence as a function of the number of steps n_{steps} leads to an overall computational cost that scales quadratically in n_{steps} (compared to the linear scaling of the state-vector simulation). Shot-based simulations are therefore significantly more computationally demanding, making the state-vector formulation of PITE indispensable for parameter exploration.

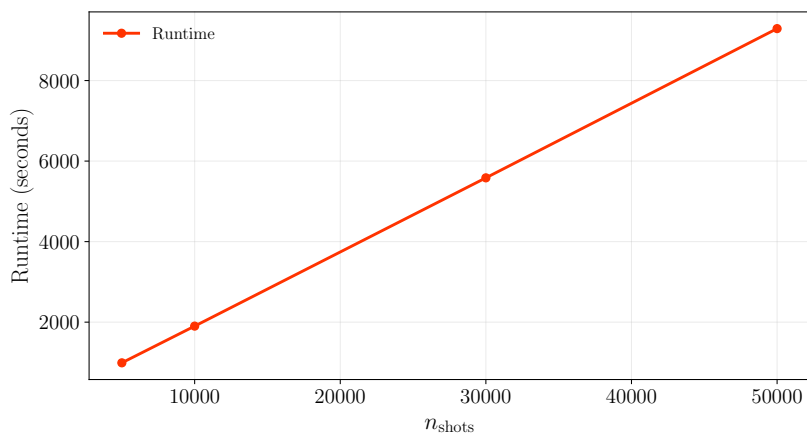


Figure 11: Runtime of shot-based PITE simulations for the $L = 16$ Heisenberg chain with $n_{\text{steps}} = 80$ steps as a function of the number of shots n_{shots} . The test was performed on a single node of the CARO high-performance computing cluster at DLR, equipped with two AMD EPYC 7702 processors with 64 cores each, i.e., 128 CPU cores in total.

C Full Code Examples

This appendix provides complete Python scripts for state-vector-based simulations, shot-based simulations, and ED simulations, as well as the full code corresponding to the basic workflow example in Sec. 4. In addition, we present different ways of constructing Hamiltonians via the PauliStringOperator interface. All scripts shown here, as well as additional examples, including the scripts used to generate the plots in this paper, are also included in the examples directory of the package available on [GitLab](#).

C.1 State-vector simulation

svPITE *Example Code 1*: State-vector-based simulation of the 1D four-site TFIM.

```
# examples/ising_4_sv.py
from svpите import PITEStatevector
from svpите.configs import PITEConfig
from svpите.operator.models import IsingHamiltonian

import matplotlib.pyplot as plt

H = IsingHamiltonian(n_sites=4, J=-1.0, h=-1.0, bc="PBC")
config = PITEConfig(gamma=0.78, n_steps=100, dt=0.1, order=1,
                    initial_state="plus")

algorithm = PITEStatevector(config, H)
result = algorithm.run(verbose=True, return_statevector=True,
                       use_qiskit_evolve=False, parallel_evolve=True)

# Print formatted result summary
print(result)

plt.plot(range(config.n_steps+1), result.energies, marker='.')
plt.title("Ising 4-site Hamiltonian Energy vs PITE Steps")
plt.xlabel("PITE Steps")
plt.ylabel("$E_0/L$")
plt.show()
```

C.2 Shot-based simulation

svPITE *Example Code 2*: Shot-based simulation of the 1D four-site TFIM.

```
# examples/ising_4_shot.py
from svpите import PITEShot
from svpите.configs import PITEConfig
from svpите.operator.models import IsingHamiltonian

import matplotlib.pyplot as plt

H = IsingHamiltonian(n_sites=4, J=-1.0, h=-1.0, bc="PBC")
config = PITEConfig(gamma=0.78, n_steps=40, dt=0.1, order=1,
                    n_shots=10000, initial_state="plus")

algorithm = PITEShot(config, H)
result = algorithm.run(verbose=True, return_circuit=True)
```

```

# Print formatted result summary
print(result)

# Draw and show the first-iteration PITE circuit
result.circuit.decompose(reps=3).draw(output="mpl")
plt.show(block=False) # Show circuit without blocking

# Plot the probability
plt.figure()
plt.plot(result.proBABILITIES[1:], marker='.')
plt.axhline(y=1.0, color='r', linestyle='--')
plt.text(0.2, 0.1, f"Energy per Site: {result.energy:.6f}\n #
    Shots: {config.n_shots}", transform=plt.gca().transAxes)
plt.xlabel("PITE step")
plt.ylabel(r"$\mathbb{P}_0$")
plt.show()

```

C.3 ED simulation

svPITE *Example Code 3*: Exact diagonalisation of the 1D four-site TFIM.

```

# examples/ising_4_ed.py
from svpите import ED
from svpите.configs import EDConfig
from svpите.operator.models import IsingHamiltonian

H = IsingHamiltonian(n_sites=4, J=-1.0, h=-1.0, bc="PBC")
spin_basis_1d_kwargs = {"kblock": 0, "pblock": 1}
# All options have default values. Here we explicitly set them
# as an example.
config = EDConfig(spin_basis_1d_kwargs=spin_basis_1d_kwargs,
                  tol=1e-10, maxiter=1000, v0=None)

algorithm = ED(config, H)
result = algorithm.run(verbose=True, return_groundstate=True)

# Print formatted result summary
print(result)

```

C.4 Hamiltonian construction

svPITE *Example Code 4*: Different ways of constructing equivalent Hamiltonians.

```
# examples/hamiltonian_construction.py
from svpите.operator import Hamiltonian, models
import numpy as np

J = -1.0
h = -1.0
bc = "PBC"

# 1. Using the predefined model
H1 = models.IsingHamiltonian(n_sites=4, J=J, h=h, bc=bc)

# 2. Generic Hamiltonian from coefficients
# (Two-site terms need boundary conditions)
terms_dict = {"ZZ": (J, bc), "X": h}
H2 = Hamiltonian(n_sites=4, terms_dict=terms_dict)

# 3. Generic Hamiltonian from coefficient arrays
J_zz = np.zeros((4,4))
for i in range(4):
    J_zz[i, (i+1)%4] = J
h_x = np.array([h for _ in range(4)])
terms_dict = {"ZZ": J_zz, "X": h_x}
H3 = Hamiltonian(n_sites=4, terms_dict=terms_dict)

# 4. Manual construction with add_term
H4 = Hamiltonian(n_sites=4, terms_dict=None)
for i in range(4):
    H4.add_term("ZZ", J, (i, (i+1)%4))
    H4.add_term("X", h, (i,))

# 5. Manual construction with add_uniform_terms
# (Two-site terms need boundary conditions)
H5 = Hamiltonian(n_sites=4, terms_dict=None)
H5.add_uniform_terms("ZZ", J, bc)
H5.add_uniform_terms("X", h)

# 6. Using a list of (coeff, sites) tuples
H6 = Hamiltonian(n_sites=4, terms_dict=None)
zz_terms = [(J, (i, (i+1)%4)) for i in range(4)]
x_terms = [(h, (i,)) for i in range(4)]
H6.add_terms_dict({"ZZ": zz_terms, "X": x_terms})

# Print and verify all Hamiltonians are equal
for i, H in enumerate([H1, H2, H3, H4, H5, H6], start=1):
    print(f"H{i}: ", H)
print("H1 == H2 == H3 == H4 == H5 == H6: ", H1 == H2 == H3 ==
      H4 == H5 == H6)
```

C.5 Basic workflow example

svPITE *Example Code 5*: Comparison of state-vector PITE, Shot-based PITE and ED

```
# examples/basic_workflow.py
# ---- Importing everything necessary ----
# Algorithms
from svpите import PITEStatevector, PITEShot, ED,
    evolve_statevector

# Configurations
from svpите.configs import PITEConfig, EDConfig

# Specific models
from svpите.operator.models import XXZHamiltonian

import numpy as np

# ---- Define model parameters ----
L = 8 # number of lattice sites
J = 1.0 / 4.0 # coupling constant
Delta = 1.0 / np.sqrt(2.0) # anisotropy
hz = 1.0 / 5.0 # external field
bc = 'PBC' # periodic boundary conditions

# ---- Define XXZ Hamiltonian in external z-field ----
# Use standard XXZ model as starting point
H = XXZHamiltonian(L, J, Delta, bc)

# Add external z-field terms to the Hamiltonian
H.add_uniform_terms("Z", hz)

# ---- Define algorithm parameters ----
config = PITEConfig(
    gamma=0.72, # Gamma parameter of the PITE algorithm
    n_steps=80, # Number of imaginary-time evolution steps
    dt=0.2, # Imaginary-time step size
    order=1, # Trotter order for the real-time evolution gate
    initial_state='singlet', # Initial state of the evolution
    n_shots=10000, # Number of shots for shot-based PITE
)

# ---- Initialize and run algorithms ----
# Statevector PITE
sv_algorithm = PITEStatevector(config, H)
sv_result = sv_algorithm.run(verbose=True, return_statevector=
    True)

# Shot-based PITE
shot_algorithm = PITEShot(config, H)
shot_result = shot_algorithm.run(verbose=True, return_circuit=
    False)
```

```

# ---- Access and print results ----
print(sv_result)
print(shot_result)

# Statevector PITE results
E_sv = sv_result.energies # Energy per site vs PITE step
P_sv = sv_result.proBABILITIES # Success probabilities vs PITE
    step

# Shot-based PITE results
E_shot = shot_result.energy # Final energy per site
dE_shot = shot_result.energy_std # Standard deviation of final
    energy per site
P_shot = shot_result.proBABILITIES # Success probabilities vs
    PITE step

# ---- Reference ED calculation ----
# Define ED configuration with symmetry sectors for the ground
    state computation
ed_basis_kwargs = {"Nup": L//2, "pblock": 1, "kblock": 0}
ed_config = EDConfig (
    tol = 1e-10, # Tolerance for eigensolver
    maxiter = 1e4, # Maximum iterations for eigensolver
    v0 = None, # Initial vector for eigensolver
    spin_basis_1d_kwargs = ed_basis_kwargs
)

# Initialize and run ED algorithm
ed_algorithm = ED(ed_config, H)
ed_result = ed_algorithm.run(verbose=True, return_groundstate=
    False)

# Access ED results
print(ed_result)
E_ed = ed_result.energy # Computed ground state energy

# ---- Beyond the Basic workflow ----
# Get the final statevector from the results
psi0 = sv_result.final_statevector

# Real-time evolution generated by H
U_dt = H.to_time_evolution_circuit(dt=1/100, reps=100, order=1)

# Evolve the PITE output state
psi_t = evolve_statevector(psi0, U_dt)

O = H.to_pauli_string_operator()
O_qiskit = O.to_sparse_pauli_op()
value_t = psi_t.expectation_value(O_qiskit)

# Access full statevector as NumPy array
psi_np = psi0.data

# Convert operator to dense matrix
O_mat = O.to_matrix(sparse=True)

```

```

# Example: expectation value using NumPy
value = np.vdot(psi_np, O_mat @ psi_np)

print("Real-time evolution successful!")

# ---- Plot results ----
import matplotlib.pyplot as plt
from matplotlib.ticker import MaxNLocator
plt.rcParams["text.usetex"] = True
plt.rcParams["text.latex.preamble"] = r"\usepackage{amsfonts}"
plt.rcParams["font.family"] = "serif"
plt.rcParams['font.size'] = 18
plt.rcParams['legend.fontsize'] = 16
plt.rcParams['xtick.labelsize'] = 16
plt.rcParams['ytick.labelsize'] = 16

cmap_red = plt.get_cmap("autumn")
cmap_blue = plt.get_cmap("winter")

fig, ax = plt.subplots(1, 2, figsize=(14, 5))

# Panel 1: PITE success probabilities
ax[0].plot(range(len(P_shot) - 1), P_shot[1:], 'o-', label='
    Shot-based PITE', color=cmap_red(0.2), markersize=3)
ax[0].plot(range(len(P_sv) - 1), P_sv[1:], 's-', label='
    Statevector PITE', color=cmap_blue(0.3), markersize=3)
ax[0].axhline(1.0, color='0.3', linestyle='--', linewidth=1)
ax[0].set_xlabel('$n_{\rm steps}$')
ax[0].set_ylabel(r'$\mathbb{P}_{0}$')
ax[0].yaxis.set_major_locator(MaxNLocator(nbins=5))
ax[0].legend(frameon=False)
ax[0].grid(True, alpha=0.25)

# Panel 2: Energy convergence
ax[1].plot(range(len(E_sv)), E_sv, 's-', label='Statevector
    PITE', color=cmap_blue(0.3), markersize=3)
ax[1].axhline(E_ed, color='black', linestyle='--', label=f'ED
    Energy = {E_ed:.4f} ')
ax[1].axhline(E_shot, color=cmap_red(0.2), linestyle='--', label
    =f'Shot-based PITE = {E_shot:.4f} $\pm$ {dE_shot:.4f}')
ax[1].fill_between(range(-5, len(E_sv)+5), E_shot - dE_shot,
    E_shot + dE_shot, alpha=0.2, color=cmap_red(0.2))
ax[1].set_xlim(-5, len(E_sv)+4)
ax[1].set_xlabel('$n_{\rm steps}$')
ax[1].set_ylabel(r'$E_0/L$')
ax[1].yaxis.set_major_locator(MaxNLocator(nbins=5))
ax[1].legend(frameon=False)
ax[1].grid(True, alpha=0.25)

for i, a in enumerate(ax):
    a.text(-0.08, 1.02, f'({chr(97+i)})',
        transform=a.transAxes,
        ha='left', va='bottom', fontsize=20)

fig.tight_layout()

```

```
fig.savefig("Basic_Workflow_Example_Panels.pdf", bbox_inches='tight', transparent=True)
plt.show()
```

References

- [1] A. Goldberg and J. L. Schwartz, *Integration of the schrödinger equation in imaginary time*, J. Comput. Phys. **1**(3), 433 (1967), doi:[10.1016/0021-9991\(67\)90049-6](https://doi.org/10.1016/0021-9991(67)90049-6).
- [2] W. M. C. Foulkes, L. Mitas, R. J. Needs and G. Rajagopal, *Quantum Monte Carlo simulations of solids*, Rev. Mod. Phys. **73**, 33 (2001), doi:[10.1103/RevModPhys.73.33](https://doi.org/10.1103/RevModPhys.73.33).
- [3] U. Schollwöck, *The density-matrix renormalization group in the age of matrix product states*, Ann. Phys. **326**(1), 96 (2011), doi:[10.1016/j.aop.2010.09.012](https://doi.org/10.1016/j.aop.2010.09.012).
- [4] S. McArdle, T. Jones, S. Endo, Y. Li, S. C. Benjamin and X. Yuan, *Variational ansatz-based quantum simulation of imaginary time evolution*, npj Quantum Inf. **5**(1), 75 (2019), doi:[10.1038/s41534-019-0187-2](https://doi.org/10.1038/s41534-019-0187-2).
- [5] X. Yuan, S. Endo, Q. Zhao, Y. Li and S. C. Benjamin, *Theory of variational quantum simulation*, Quantum **3**, 191 (2019), doi:[10.22331/q-2019-10-07-191](https://doi.org/10.22331/q-2019-10-07-191).
- [6] M. Motta, C. Sun, A. T. K. Tan, M. J. O'Rourke, E. Ye, A. J. Minnich, F. G. S. L. Brandão and G. K.-L. Chan, *Determining eigenstates and thermal states on a quantum computer using quantum imaginary time evolution*, Nat. Phys. **16**(2), 205 (2019), doi:[10.1038/s41567-019-0704-4](https://doi.org/10.1038/s41567-019-0704-4).
- [7] S.-H. Lin, R. Dilip, A. G. Green, A. Smith and F. Pollmann, *Real- and Imaginary-Time Evolution with Compressed Quantum Circuits*, PRX Quantum **2**(1), 010342 (2021), doi:[10.1103/PRXQuantum.2.010342](https://doi.org/10.1103/PRXQuantum.2.010342).
- [8] T. Kosugi, Y. Nishiya, H. Nishi and Y.-i. Matsushita, *Imaginary-time evolution using forward and backward real-time evolution with a single ancilla: First-quantized eigen-solver algorithm for quantum chemistry*, Phys. Rev. Research **4**(3), 033121 (2022), doi:[10.1103/PhysRevResearch.4.033121](https://doi.org/10.1103/PhysRevResearch.4.033121).
- [9] H. Nishi, K. Hamada, Y. Nishiya, T. Kosugi and Y.-i. Matsushita, *Optimal scheduling in probabilistic imaginary-time evolution on a quantum computer*, Phys. Rev. Research **5**(4), 043048 (2023), doi:[10.1103/PhysRevResearch.5.043048](https://doi.org/10.1103/PhysRevResearch.5.043048).
- [10] S. Ejima, K. Seki, B. Fauseweh and S. Yunoki, *Probabilistic imaginary-time evolution in state-vector-based and shot-based simulations and on quantum devices*, Phys. Rev. Research **7**, 043182 (2025), doi:[10.1103/2s2p-kvcx](https://doi.org/10.1103/2s2p-kvcx).
- [11] P. Weinberg and M. Bukov, *QuSpin: A Python package for dynamics and exact diagonalisation of quantum many body systems part I: Spin chains*, SciPost Phys. **2**(1), 003 (2017), doi:[10.21468/SciPostPhys.2.1.003](https://doi.org/10.21468/SciPostPhys.2.1.003).
- [12] A. Javadi-Abhari, M. Treinish, K. Krsulich, C. J. Wood, J. Lishman, J. Gacon, S. Martiel, P. D. Nation, L. S. Bishop, A. W. Cross, B. R. Johnson and J. M. Gambetta, *Quantum computing with Qiskit*, doi:[10.48550/arXiv.2405.08810](https://doi.org/10.48550/arXiv.2405.08810) (2024), [arXiv:2405.08810](https://arxiv.org/abs/2405.08810).
- [13] H. F. Trotter, *On the product of semi-groups of operators*, Proc. Amer. Math. Soc. **10**(4), 545–551 (1959), doi:[10.1090/s0002-9939-1959-0108732-6](https://doi.org/10.1090/s0002-9939-1959-0108732-6).

- [14] M. Suzuki, *Relationship between d -dimensional quantal spin systems and $(d+1)$ -dimensional Ising systems: Equivalence, critical exponents and systematic approximants of the partition function and spin correlations*, Prog. Theor. Phys. **56**(5), 1454–1469 (1976), doi:[10.1143/ptp.56.1454](https://doi.org/10.1143/ptp.56.1454).
- [15] A. W. Sandvik, *Finite-size scaling of the ground-state parameters of the two-dimensional Heisenberg model*, Phys. Rev. B **56**(18), 11678–11690 (1997), doi:[10.1103/physrevb.56.11678](https://doi.org/10.1103/physrevb.56.11678).
- [16] A. W. Sandvik, *High-precision ground state parameters of the two-dimensional spin-1/2 Heisenberg model on the square lattice*, doi:[10.48550/arxiv.2601.20189](https://doi.org/10.48550/arxiv.2601.20189) (2026), [arXiv:2601.20189](https://arxiv.org/abs/2601.20189).
- [17] R. Seidel, S. Bock, R. Zander, M. Petrič, N. Steinmann, N. Tcholchev and M. Hauswirth, *Qrisp: A framework for compilable high-level programming of gate-based quantum computers*, doi:[10.48550/arxiv.2406.14792](https://doi.org/10.48550/arxiv.2406.14792) (2024), [arXiv:2406.14792](https://arxiv.org/abs/2406.14792).
- [18] S. V. Isakov, D. Kafri, O. Martin, C. V. Heidweiller, W. Mruczkiewicz, M. P. Harrigan, N. C. Rubin, R. Thomson, M. Broughton, K. Kissell, E. Peters, E. Gustafson *et al.*, *Simulations of quantum circuits with approximate noise using qsim and cirq*, doi:[10.48550/arxiv.2111.02396](https://doi.org/10.48550/arxiv.2111.02396) (2021), [arXiv:2111.02396](https://arxiv.org/abs/2111.02396).
- [19] Y. Suzuki, Y. Kawase, Y. Masumura, Y. Hiraga, M. Nakadai, J. Chen, K. M. Nakanishi, K. Mitarai, R. Imai, S. Tamiya, T. Yamamoto, T. Yan *et al.*, *Qulacs: a fast and versatile quantum circuit simulator for research purpose*, Quantum **5**, 559 (2021), doi:[10.22331/q-2021-10-06-559](https://doi.org/10.22331/q-2021-10-06-559).
- [20] V. Bergholm, J. Izaac, M. Schuld, C. Gogolin, S. Ahmed, V. Ajith, M. S. Alam, G. Alonso-Linaje, B. AkashNarayanan, A. Asadi, J. M. Arrazola, U. Azad *et al.*, *Pennylane: Automatic differentiation of hybrid quantum-classical computations*, doi:[10.48550/arxiv.1811.04968](https://doi.org/10.48550/arxiv.1811.04968) (2018), [arXiv:1811.04968](https://arxiv.org/abs/1811.04968).